Integrative model-based comparison of target site-specific antimicrobial effects: a case study with ceftaroline and lefamulin

Os, W. van; Pham, A.D.; Eberl, S.; Minichmayr, I.K.; Hasselt, J.G.C. van; Zeitlinger, M.

International Journal of Antimicrobial Agents 63 (2024) 107148

Contents lists available at ScienceDirect

International Journal of Antimicrobial Agents

journal homepage: www.elsevier.com/locate/ijantimicag

Integrative model-based comparison of target site-specific antimicrobial effects: A case study with ceftaroline and lefamulin

Wisse van Os[a], Anh Duc Pham[b], Sabine Eberl[a], Iris K. Minichmayr[a], J.G. Coen van Hasselt[b], Markus Zeitlinger[a,*]

[a] Department of Clinical Pharmacology, Medical University of Vienna, Vienna, Austria
[b] Division of Systems Pharmacology & Pharmacy, Leiden Academic Centre for Drug Research, Leiden University, Leiden, Netherlands

ARTICLE INFO

Article history:
Received 31 July 2023
Accepted 14 March 2024

Editor: G. Rao

Keywords:
PK-PD
Pharmacometrics
Target site
Microdialysis
Ceftaroline
Lefamulin

ABSTRACT

Objective: Predictions of antimicrobial effects typically rely on plasma-based pharmacokinetic-pharmacodynamic (PK-PD) targets, ignoring target-site concentrations and potential differences in tissue penetration between antibiotics. In this study, we applied PK-PD modelling to compare target site-specific effects of antibiotics by integrating clinical microdialysis data, in vitro time-kill curves, and antimicrobial susceptibility distributions. As a case study, we compared the effect of lefamulin and ceftaroline against methicillin-resistant *Staphylococcus aureus* (MRSA) at soft-tissue concentrations.

Methods: A population PK model describing lefamulin concentrations in plasma, subcutaneous adipose and muscle tissue was developed. For ceftaroline, a similar previously reported PK model was adopted. In vitro time-kill experiments were performed with six MRSA isolates and a PD model was developed to describe bacterial growth and antimicrobial effects. The clinical PK and in vitro PD models were linked to compare antimicrobial effects of ceftaroline and lefamulin at the different target sites.

Results: Considering minimum inhibitory concentration (MIC) distributions and standard dosages, ceftaroline showed superior anti-MRSA effects compared to lefamulin both at plasma and soft-tissue concentrations. Looking at the individual antibiotics, lefamulin effects were highest at soft-tissue concentrations, while ceftaroline effects were highest at plasma concentrations, emphasising the importance of considering target-site PK-PD in antibiotic treatment optimisation.

Conclusion: Given standard dosing regimens, ceftaroline appeared more effective than lefamulin against MRSA at soft-tissue concentrations. The PK-PD model-based approach applied in this study could be used to compare or explore the potential of antibiotics for specific indications or in populations with unique target-site PK.

1. Introduction

Comparing predictions of antimicrobial effect for different drugs based on traditional pharmacokinetic/pharmacodynamic (PK/PD) indices (e.g., the ratio of area under the curve to minimum inhibitory concentration [AUC/MIC]), and probability of target attainment (PTA) analyses has several limitations. First, PK/PD targets and PTA analyses are typically based on plasma PK and do not consider drug distribution to peripheral infection sites. Not only might an antibiotic be unequally distributed from blood to different tissues; penetration to a specific tissue might also markedly differ between antibiotics [1]. Moreover, disease states such as sepsis may affect tissue penetration of different antibiotics to a different extent [2,3]. Therefore, basing antibiotic treatment selection for specific indications or patient populations solely on plasma drug exposures may be suboptimal with respect to treatment success or toxicity [2,4]. Second, the PK/PD targets may have been derived using different pathogens, different types of data (e.g., from murine infection models, in vitro time-kill experiments, or clinical studies), or PD endpoints (e.g., bacteriostasis, log-reduction in bacterial count, or clinical cure), thus complicatingcomparisons between antibiotics. Third, PK/PD targets are summary endpoints that capture only one specific time point and thus provide no information on the time course of antibiotic concentrations and effects [5]. PTA analyses further reduce dynamic and continuous PK and PD

* Corresponding author: Markus Zeitlinger, Department of Clinical Pharmacology, Medical University of Vienna, Währinger Gürtel 18-20, 1090 Vienna, Austria. Tel.: +43 (0)1 40400-29800; fax: +43 (0)1 40400-29980
E-mail address: markus.zeitlinger@meduniwien.ac.at (M. Zeitlinger).

https://doi.org/10.1016/j.ijantimicag.2024.107148

processes to a dichotomous outcome, i.e., whether a threshold value is achieved, and do not provide insight into the exact magnitude of antimicrobial effects.

To address these limitations, this study demonstrates how PK-PD modelling can be applied to compare the target-site PK-PD of two antibiotics through integrating i) continuous time courses of target-site concentrations, ii) continuous time courses of antimicrobial effects against a pathogen relevant for the indication of interest, and iii) antimicrobial susceptibility distributions for that pathogen. As a case study, we compare the effect of ceftaroline and lefamulin at soft-tissue concentrations against methicillin-resistant *Staphylococcus aureus* (MRSA). Ceftaroline is a cephalosporin antibiotic approved for the treatment of complicated skin and skin-structure infections (cSSSIs) and community-acquired bacterial pneumonia (CABP). Plasma PK-based PTA analyses suggested better MRSA coverage of ceftaroline compared to other antibiotics commonly used to treat skin and soft-tissue infections (SSTIs) [6,7]. Lefamulin is a pleuromutilin antibiotic approved for the treatment of CABP. Considering its spectrum of activity and low potential for cross-resistance with other antibiotic classes, lefamulin may have potential for the treatment of SSTIs [8]. In a proof-of-concept phase-2 trial in patients with acute bacterial skin and skin-structure infections (ABSSSIs), lefamulin was non-inferior to vancomycin [9]. If lefamulin demonstrated antimicrobial activity comparable or superior to ceftaroline at soft-tissue concentrations against MRSA, one of the predominant and most difficult-to-treat pathogens causing SSTIs [10,11], that would add to the data suggesting its potential as a treatment option for SSTIs.

This study thus aimed to demonstrate how PK-PD modelling can be applied to compare target site-specific PK-PD of antibiotics using data relating to the soft-tissue PK-PD of lefamulin and ceftaroline. For this purpose, we employed population PK models for concentration-time profiles in plasma and subcutaneous adipose and skeletal muscle tissue. We also performed in vitro time-kill experiments with six MRSA isolates and developed a PD model to quantify MIC-dependent concentration-effect relationships of the two drugs against MRSA. The PK and PD models were then coupled to simulate bacterial response to dynamic drug concentrations in plasma and soft tissues over time, also considering clinical MIC distributions for MRSA. Based on the integrated PK-PD data, our study sought to determine which of the two treatments may be more effective against MRSA in soft-tissue infections.

2. Methods

2.1. PK model for lefamulin

To describe lefamulin concentration-time profiles in plasma and subcutaneous adipose and skeletal muscle tissue, a population PK model was developed based on observations from a previous study [12]. Briefly, twelve healthy volunteers received a single dose of 150 mg lefamulin as intravenous infusion over 1 h. Microdialysis was used to quantify unbound concentrations in the interstitial space fluid (ISF) of soft tissues over a period of 24 h. Total plasma concentrations were also quantified. A total of 144 plasma and 249 interstitial concentrations were used in the analysis. Observations below the quantification limit (0.001 mg/L) comprised 2.2% of observations and were omitted due to minimal impact on parameter estimates as previously shown [13].

First, the population PK model for plasma was developed. One-, two- and three-compartment models with first-order elimination were evaluated. A previously reported saturable protein binding model for lefamulin was incorporated in the model to convert total to unbound plasma concentrations [14].

Microdialysis data were modelled using an integrated dialysate-based approach, which considers the time interval of dialysate collection and uses measured dialysate concentrations as input for the model, rather than correcting for relative recovery before the analysis [15]. To describe tissue distribution, (i) models in which concentrations of the plasma compartments were scaled to ISF concentrations, and (ii) models with separate tissue compartments for subcutaneous adipose and/or muscle tissue were evaluated. For models with separate tissue compartments, we also evaluated estimating separate clearance parameters for distribution into and out of the tissue compartments, non-linear tissue distribution, and models with multiple tissue compartments (e.g., a 'shallow' and 'deep' compartment for one tissue).

Inter-individual variability was investigated for all structural model PK parameters which were assumed to follow a log-normal distribution. To describe residual unexplained variability (RUV), proportional, additive and combined error models were evaluated separately for plasma, microdialysate and retrodialysate concentrations. Covariate analyses were not performed considering the small size and homogeneity of the study population and given that previous population PK analyses with larger and more diverse populations did not identify significant parameter-covariate relationships [14,16].

2.2. PK model for ceftaroline

Concentration-time profiles of ceftaroline were simulated using a previously reported population PK model describing exposure in plasma, subcutaneous adipose tissue, muscle tissue and cerebrospinal fluid (CSF) [17]. Part of the data underlying the model had been obtained in a microdialysis study with 12 healthy volunteers [18] that was performed in the same hospital and with a design similar to the aforementioned lefamulin PK study [12]. In the model, ceftaroline tissue concentrations were described using one peripheral compartment per tissue with separate clearance parameters describing distribution into and out of these compartments. Total body weight, creatinine clearance (CrCl; calculated with the Cockcroft-Gault equation), type of study participant (healthy volunteers and neurosurgical patients) and CSF glucose concentrations were included as covariates [17]. To create a population with similar characteristics as the population in the lefamulin microdialysis study [12], ceftaroline PK was simulated for healthy subjects with normal renal function (CrCl 90–150 mL/min) and a body weight of 60–100 kg, assuming uniform distributions of the two characteristics within these ranges. CSF glucose levels were set to 3.9 mmol/L, corresponding to the median value in the population underlying model development [19]. In line with previous studies, ceftaroline doses were corrected based on the differences in molecular weight between ceftaroline and its prodrug ceftaroline fosamil, since the PK model assumed instantaneous prodrug-to-drug conversion [17,20], e.g., 600 mg ceftaroline fosamil corresponded to 530 mg ceftaroline.

2.3. In vitro time-kill experiments

To allow the characterisation of concentration-effect relationships, time-kill studies with ceftaroline (ceftaroline dihydrochoride; AstraZeneca Österreich, Vienna, Austria) and lefamulin (Xenleta®; Pharmore GmbH, Ibbenbüren, Germany) were performed in triplicates with six MRSA strains (ATCC 33592, DSM 23622, and four clinical strains isolated from SSTIs at the Vienna General Hospital). MIC values were determined using broth microdilution [21]. A log-phase bacterial culture was inoculated in 5 mL of pre-warmed (37°C) cation-adjusted Mueller Hinton Broth (CAMHB; Sigma-Aldrich, Vienna, Austria) to reach an initial bacterial population of $\sim 10^6$ colony forming units (CFU)/mL. Bacteria were exposed to seven drug concentrations ranging from 0.125 to 8 times the MIC of the respective strain in twofold increments.

Growth controls were also performed. To determine bacterial concentrations, samples were taken at 0 (pre-exposure), 2, 4, 6, 8, 10 and 24 h after inoculation, serially diluted in 0.9% saline and plated using 20 μL drops on Columbia agar plates with 5% sheep blood (bioMérieux, Marcy-l'Etoile, France). Bacterial colonies were counted after overnight incubation at 37°C in ambient air.

2.4. PD model development

A PD model was developed based on the time-kill data to mathematically describe bacterial growth and antimicrobial effects. First, the data for each of the six bacterial strains as well as for each of the two antibiotics were modelled separately. Bacterial growth was described with a first-order rate constant and limited by the estimated maximum bacterial population size. Linear, power and sigmoid E_{max} models were evaluated to describe antibiotic concentration-effect relationships. Bacterial regrowth was evaluated using concentration-dependent rates of reduction in potency (EC_{50}) [22] or maximum kill rate (E_{max}) [23], as well as by including a less susceptible subpopulation (compartment) in the model. Observations below the limit of detection (LOD; 50 CFU/mL) were handled according to the M3 method, i.e., by estimating the probability that a measurement is below the LOD [13]. Bacterial concentrations were log-transformed and additive error models were used to describe RUV. In the next step, time-kill data produced for the same antibiotic (i.e., ceftaroline or lefamulin), were jointly modelled to create a single model describing antimicrobial effects against all MRSA strains. Thereby, the MIC was tested as a potentially influential factor (i.e., covariate) causing variability between strains in exposure-response parameters (e.g., EC_{50}) using linear and power functions [23–26]. Finally, estimates of bacteria-related parameters (initial and maximum population size, growth rate) were shared for the two drugs to create a combined model.

2.5. Antibiotic stability

Previously reported data on ceftaroline stability in MHB at 37°C [27] were used to estimate a zero-order drug degradation rate, which was incorporated in the PD model. To evaluate whether degradation of lefamulin occurred in the time-kill experiments, we evaluated the stability of its effect in an additional time-kill experiment. Briefly, one set of tubes (n = 12) containing lefamulin at concentrations of 0.5, 1, or 2 times the MIC (n = 4 replicates) was immediately inoculated with the strain ATCC 33592. A second set of tubes containing the same lefamulin concentrations was pre-incubated for 24 h under the same conditions prior to inoculation. Observations from the experiments with and without pre-incubation were compared to detect any loss of effect. As a control, these experiments were also performed with ceftaroline.

2.6. Model evaluation

Evaluation and selection of the PK and PD models were based on graphical and statistical criteria including the objective function value (OFV), for which a decrease of >3.84 points was considered statistically significant (α = 0.05) for nested models with one additional degree of freedom. The Akaike information criterion (AIC) was used to compare non-nested models. Furthermore, the precision of parameter estimates, goodness-of-fit plots and visual predictive checks (VPCs; n = 1000) were assessed [28].

2.7. Bacterial response simulations

To compare the antimicrobial effects of ceftaroline and lefamulin given dynamic unbound concentrations in plasma and soft tissues, the population PK and in vitro PD models were linked (Figure 1) and simulations were performed (n = 1000 subjects per MIC value). Only inter-individual PK variability was considered in the Monte-Carlo simulations (not the RUV in PK and PD). For simulations of bacterial response, the initial bacterial population size was set to 10^6 CFU/mL. The bacterial count at 24 h was used as a metric to compare the effect of the two antibiotics.

2.8. Software

All modelling and simulation activities were performed with NONMEM 7.4 (ICON plc, Gaithersburg, MD, USA) using first-order conditional estimation method with interaction for the lefamulin PK model and Laplacian estimation with interaction for the PD model, aided by PsN (v5.3.0; Uppsala University, Uppsala, Sweden) [29] and Pirana (v21.11.1; Certara, Princeton, NJ, USA) [30]. R (v4.0.3) [31] was used for data processing and visualisation.

3. Results

3.1. Population PK model lefamulin

The plasma PK of lefamulin was best described with a three-compartment model, in accordance with previously reported population PK models [14,16]. Soft-tissue PK was best described by a model with two additional compartments for each tissue (Figure 1), potentially reflecting intracellular distribution of lefamulin [32]. Single compartments for subcutaneous adipose and muscle tissue or scaling concentrations in the central or peripheral compartments of the plasma model to ISF concentrations resulted in model misspecification (visible in graphical evaluations of conditional weighted residuals). To enhance model stability, the volumes of distribution of the ISF compartments were fixed to previously reported physiological values [33], an approach that had also been taken for the ceftaroline model [17]. Parameters were estimated with acceptable precision (Table 1) and the final model adequately described both plasma and soft-tissue PK (Figure 2, Figure S1).

3.2. Simulations of antibiotic PK

Unbound drug concentration-time courses in plasma and soft tissues were simulated for a virtual population using the PK models for lefamulin and ceftaroline. The equations for both PK models are reported in the Supplementary material. The simulated PK profiles following standard dosages of lefamulin (150 mg q12h infused over 1 h) and ceftaroline fosamil (600 mg q12 h infused over 1 h) are depicted in Figure S2. The AUC-based penetration ratios ($AUC_{0\text{-}24h,tissue}/AUC_{0\text{-}24h,plasma}$) in the simulated population were lower and more variable for ceftaroline (median 0.58 [90% prediction interval 0.33–1.00] and 0.52 [0.32–0.84]) than for lefamulin (0.94 [0.86–0.98] and 0.94 [0.77–0.98] for subcutaneous adipose and skeletal muscle tissue, respectively). Lefamulin thus penetrates more extensively into soft tissues than ceftaroline.

3.3. Time-kill experiments

The antimicrobial effects of the two drugs against MRSA across a range of concentrations were followed over time using in vitro time-kill experiments. The investigated bacterial strains displayed MIC values of lefamulin and ceftaroline that included the most commonly reported values for MRSA according to EUCAST (European Committee on Antimicrobial Susceptibility Testing) (Table 2) [34]. More precisely, the MIC values in our study cover 92% and

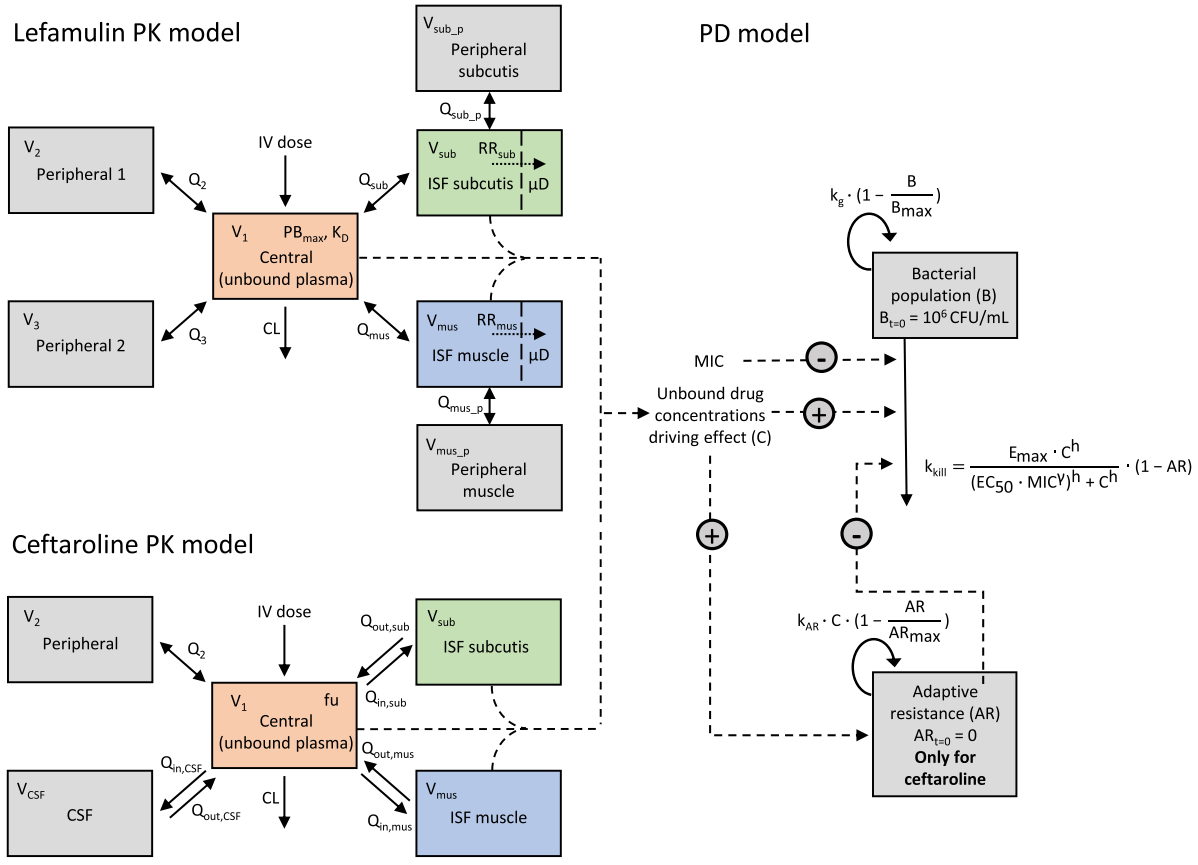

Figure 1. Structure of the combined PK-PD model used for simulations, together with the estimated parameters. Solid lines represent mass transfers; dashed lines indicate how model components are related. PK: pharmacokinetic, PD: pharmacodynamic; IV: intravenous; CSF: cerebrospinal fluid; μD: microdialysate; fu: unbound fraction; k_{kill}: rate of bacterial killing. Explanations of other abbreviations are provided in Tables 1 and 3.

Table 1
Parameter estimates of the lefamulin population pharmacokinetic model.

Parameter	Description	Estimate (%RSE)	IIV in CV% (%RSE)
CL (L/h)	Clearance	137 (6.2)	21.5 (20.9)
V_1 (L)	Volume of distribution of the central compartment	75.7 (5.2)	
Q_2 (L/h)	Intercompartmental clearance between the central and first peripheral compartment	42.9 (23.3)	64.8 (23.6)
V_2 (L)	Volume of distribution of the first peripheral compartment	391 (12.4)	32.8 (31.5)
Q_3 (L/h)	Intercompartmental clearance between the central and second peripheral compartment	218 (6.4)	15.7 (31.9)
V_3 (L)	Volume of distribution of the second peripheral compartment	400 (7.0)	
PB_{max} (mg/L)	Maximum plasma protein binding capacity	12.7 (fixed)	
K_D (mg/L)	Plasma protein dissociation constant	2.07 (fixed)	
Q_{sub} (L/h)	Intercompartmental clearance between the central and s.c. ISF compartment	2.16 (15.6)	
V_{sub} (L)	Volume of distribution of the s.c. ISF compartment	2.29 (fixed)	
Q_{mus} (L/h)	Intercompartmental clearance between the central and muscle ISF compartment	2.04 (20.5)	
V_{mus} (L)	Volume of distribution of the muscle ISF compartment	3.91 (fixed)	
Q_{sub_p} (L/h)	Intercompartmental clearance between the s.c. ISF and the peripheral s.c. compartment	0.623 (20.9)	51.0 (24.5)
V_{sub_p} (L)	Volume of distribution of the peripheral s.c. compartment	2.79 (22.8)	
Q_{mus_p} (L/h)	Intercompartmental clearance between the muscle ISF and the peripheral muscle compartment	0.52 (41.3)	74.4 (23.4)
V_{mus_p} (L)	Volume of distribution of the peripheral muscle compartment	1.80 (30.7)	
RR_{sub} (%)	Relative recovery of microdialysis in s.c. ISF	14.5 (17.0)	64.2 (20.7)
RR_{mus} (%)	Relative recovery of microdialysis in muscle ISF	21.0 (6.3)	20.4 (23.9)
RUV_{plasma} (%)	Proportional RUV – plasma observations	9.26 (7.6)	
$RUV_{\mu D\_sub}$ (%)	Proportional RUV – microdialysate observations in s.c. tissue	19.9 (7.5)	
$RUV_{\mu D\_mus}$ (%)	Proportional RUV – microdialysate observations in muscle tissue	22.5 (7.3)	
RUV_{RD_sub} (%)	Proportional RUV – retrodialysate observations in s.c. tissue	11.9 (14.7)	
RUV_{RD_mus} (%)	Proportional RUV – retrodialysate observations in muscle tissue	13.8 (16.0)	

RSE: relative standard error; IIV: inter-individual variability; CV: coefficient of variation, calculated according to $\sqrt{e^{\omega^2}-1}\times$ 100%; s.c.: subcutaneous; ISF: interstitial space fluid; RUV: residual unexplained variability.
Estimates are based on unbound drug concentrations. For parameter estimates of the ceftaroline PK model, the reader is referred to Helfer et al. [17].

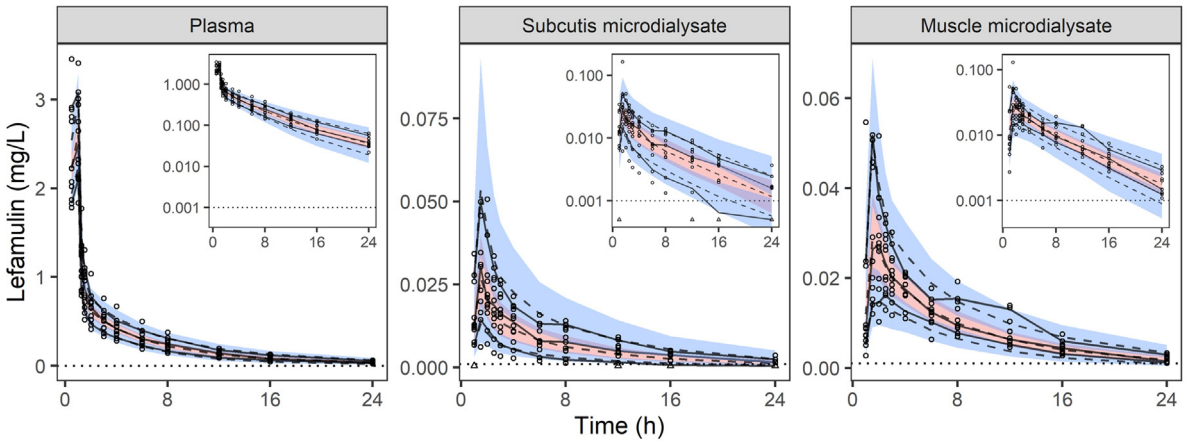

Figure 2. Visual predictive check for the lefamulin population pharmacokinetic model on linear and log-scale (inserts). Circles represent observations. The solid and dashed lines represent the 10th, 50th and 90th percentiles of observed and simulated data, and the shaded areas indicate the 95% confidence intervals around the simulated percentiles. The dotted line indicates the lower limit of quantification (LLOQ; 0.001 mg/L). Observations <LLOQ were excluded from the modelling dataset but are plotted as triangles at a value of LLOQ/2. One observation in the microdialysate of subcutaneous adipose tissue (0.16 mg/L) and one observation in muscle tissue microdialysate (0.13 mg/L), both at 1.5 h, are not shown in the plots with linear scale for the sake of legibility.

Table 2
MIC values of the isolates used in the study.

Isolate	MIC (mg/L)	
	Lefamulin	Ceftaroline
563	0.25	0.5
692	0.06	0.5
784	0.125	0.25
845	0.25	0.5
ATCC 33592	0.125	1
DSM 23622	0.125	2

ATCC: American Type Culture Collection; DSM: German Collection of Microorganisms; MIC: minimum inhibitory concentration.

93% of the lefamulin and ceftaroline MIC values reported by EUCAST for MRSA, respectively [34].

At high concentrations relative to the MIC, ceftaroline killed MRSA faster than lefamulin (Figure 3; see Figure S3 for raw time-kill curves). A decrease in effect over time was observed over 24 h for ceftaroline but not for lefamulin. Considering drug concentrations relative to the MIC, results were similar for all strains, with the highest variability observed at concentrations around the MIC (Figure S3). Results were consistent between replicate experiments.

The stability experiments revealed no decrease in the antimicrobial effect of lefamulin after 24 h of pre-incubation, in contrast to ceftaroline (Figure S4). Hence, the lefamulin degradation rate constant in the PD model was fixed to 0.

3.4. PD model

Next, a PD model was developed based on all time-kill data to allow the prediction of antimicrobial effects given human PK profiles. Sigmoid E_{max} models best described the in vitro effect of both antibiotics. A concentration-dependent reduction of the E_{max} over time, the extent of which was limited by a parameter representing the maximum fractional reduction of drug effect, was empirically selected to describe the observed regrowth following ceftaroline exposure (Table 3) [23]. An adaptive resistance function increasing the EC_{50} [22] did not capture the regrowth well (ΔAIC = 103 compared to the E_{max} reduction model), and assuming a less susceptible subpopulation in the inoculum led to convergence issues. For both drugs, the inclusion of MIC as a covariate on EC_{50} was required to describe the data from all strains simultaneously (ΔOFV = 385 and 881 for lefamulin and ceftaroline, respectively). A power function was subsequently found to be statistically superior to a linear relationship (ΔOFV = 102 and 36.4 for lefamulin and ceftaroline, respectively). The final combined model overall adequately described the observed time-kill curves (Figure 3, Figure S5). The rapid killing of isolates 692 and 845 at ceftaroline concentrations $\geq 4 \cdot$ MIC and the extent of the regrowth observed for

Table 3
Parameter estimates of the in vitro pharmacodynamic model.

Parameter	Description	Estimate (%RSE)	
		Lefamulin	Ceftaroline
CFU_{t0} (log_{10} CFU/mL)	Initial inoculum size in time-kill experiments	5.87 (0.3)	
k_g (h^{-1})	Bacterial growth rate constant	1.01 (2.9)	
B_{max} (log_{10} CFU/mL)	Maximum bacterial density	8.57 (0.4)	
E_{max} (h^{-1})	Maximum drug effect rate constant	1.19 (2.4)	2.37 (4.1)
EC_{50} (mg/L·MIC$^{\gamma}$)	Drug concentration at which effect is half-maximal, MIC-dependent	0.308 (6.3)	0.549 (3.2)
h	Hill coefficient in drug effect equation	2.66 (4.5)	1.76 (5.4)
γ	Covariate describing power relationship between MIC and EC_{50}	0.712 (3.9)	0.841 (2.9)
k_{AR} (L/mg·h^{-1})	Rate constant of adaptive resistance development	-	0.108 (18.2)
AR_{max}	Maximum fractional reduction in drug effect due to adaptive resistance	-	0.44 (5.3)
k_{deg} (h^{-1})	Drug degradation rate in vitro (zero-order)	0 (fixed)	-0.012 (5.4)
RUV_{add} (log_{10} CFU/mL)	Additive residual unexplained variability (standard deviation)	0.389 (2.3)	0.605 (2.3)

RSE: relative standard error; CFU: colony-forming units; MIC: minimum inhibitory concentration.

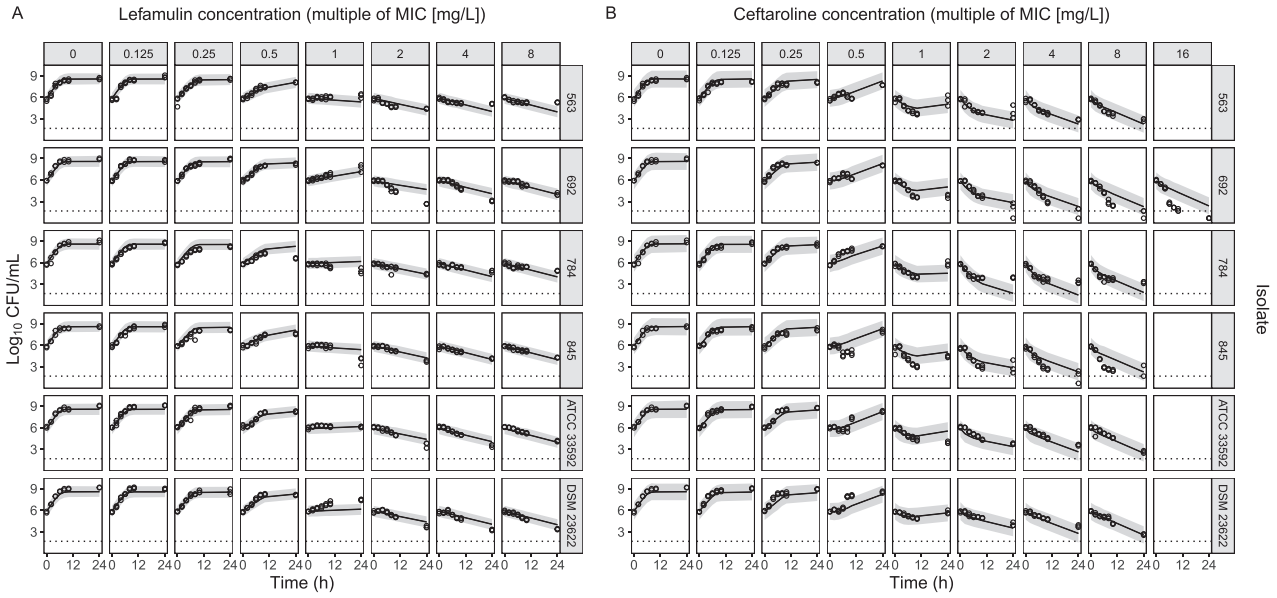

Figure 3. Visual predictive check for the in vitro pharmacodynamic model for lefamulin (A) and ceftaroline (B). Symbols represent observations. Solid lines represent median values of simulations (n = 1000), and the shaded areas show the 95% prediction intervals. The dotted line represents the limit of detection (LOD; 50 CFU/mL). Observations <LOD are plotted at a value of $\log_{10}$(LOD)/2. MIC: minimum inhibitory concentration; CFU: colony-forming units; ATCC: American Type Culture Collection; DSM: German Collection of Microorganisms.

isolate 784 were less well captured. The equations of the final PD model are reported in the supplementary material.

3.5. Simulations of target-site antimicrobial effect

Finally, the clinical PK and in vitro PD models were linked to simulate bacterial response to dynamic unbound drug concentrations in plasma and soft tissues. Simulations with commonly observed MIC values for MRSA showed that standard doses of ceftaroline fosamil resulted in lower bacterial counts at 24 h than standard doses of lefamulin, regardless of whether simulations were based on unbound plasma or soft-tissue concentration-time profiles (Figure 4). The simulated PK-PD profiles of ceftaroline were more variable than those of lefamulin as a result of the higher inter-individual variability in ceftaroline PK. The antimicrobial effect of lefamulin was highest at soft-tissue concentrations. In contrast, the effect of ceftaroline was highest at plasma concentrations (Figure 4). The full time courses of the PD simulations are depicted in Figure S6.

Simulations were also used to explore which lefamulin dose was required to achieve an effect corresponding to that of a standard dosing regimen of ceftaroline against a pathogen with MIC_{90} (MRSA) for each antibiotic (Figure 5) [34]. Due to the more extensive soft-tissue penetration of lefamulin compared to ceftaroline, lefamulin doses required to attain an effect equivalent to the bacterial killing caused by standard doses of ceftaroline were lower when bacterial response was driven by soft-tissue PK (~300 mg q12h) compared to plasma PK (~575 mg q12h) [34], but still above the currently licensed maximum dosage of 150 mg q12 h.

4. Discussion

Comparing effect predictions for different antibiotics is challenging as PK/PD index targets are commonly not based on concentrations at the target site and, being derived using varying methods and a fragmented workflow, do not allow for direct comparisons of antibiotic effects. This may lead to suboptimal treatment for a specific infection type or patient population. In this study, we demonstrated how PK-PD modelling can be leveraged to directly compare the effect of two antibiotics at target-site concentrations. As a case study, we compared the effect of lefamulin and ceftaroline against MRSA at concentrations in interstitial subcutaneous adipose and skeletal muscle tissue.

Given standard dosages and considering the MRSA MIC distributions for both antibiotics, bacterial killing following exposure to soft-tissue concentrations was higher for ceftaroline compared to lefamulin. Substantial dose increases of lefamulin, which are currently not supported by safety data [35], would be required to match the effect of ceftaroline. Differences in antimicrobial effects between the two drugs were smaller based on soft-tissue PK compared to plasma PK. This can be explained by the more extensive distribution of lefamulin into soft tissues, as shown by the simulations in the present study and the previously reported AUC-based tissue penetration ratios obtained in the microdialysis studies (lefamulin: 0.98 and 0.87; ceftaroline: 0.53 and 0.50 for subcutaneous adipose and muscle tissue, respectively) [12,18]. These results emphasise the importance of considering target-site PK-PD in treatment selection and dose optimisation.

The effect against MRSA of both drugs appeared lower in this study compared to plasma PK-based PTA analyses based on preclinical PK/PD targets [17,36,37]. Given the same dosages as in our simulations, these previous analyses found a PTA ≥90% (i) for ceftaroline MIC values ≤2 mg/L when based on a PK/PD target reflecting a 2-log bacterial reduction over 24 h [17,36], and (ii) for lefamulin MIC values ≤0.06 mg/L when based on a PK/PD target reflecting bacteriostasis over 24 h [37]. Looking at the median values of the PK-PD simulations over 24 h in the present study, the same PD endpoints (i.e., a 2-log bacterial reduction for ceftaroline and bacteriostasis for lefamulin) were achieved only at lower MIC values. Additionally, simulations with the most commonly occurring lefamulin MIC values indicated a net bacterial growth over 24 h, while a phase-2 trial of lefamulin in patients with ABSSSIs reported high clinical cure rates [9]. The discrepancies between our results and the PTA analyses and/or clinical cure results could be due to several potential reasons. First, bacterial growth rates can be higher in vitro in rich growth media than in vivo [38]. Second, host factors, notably immune system components, are absent in in vitro time-kill experiments but play a role in bacterial growth

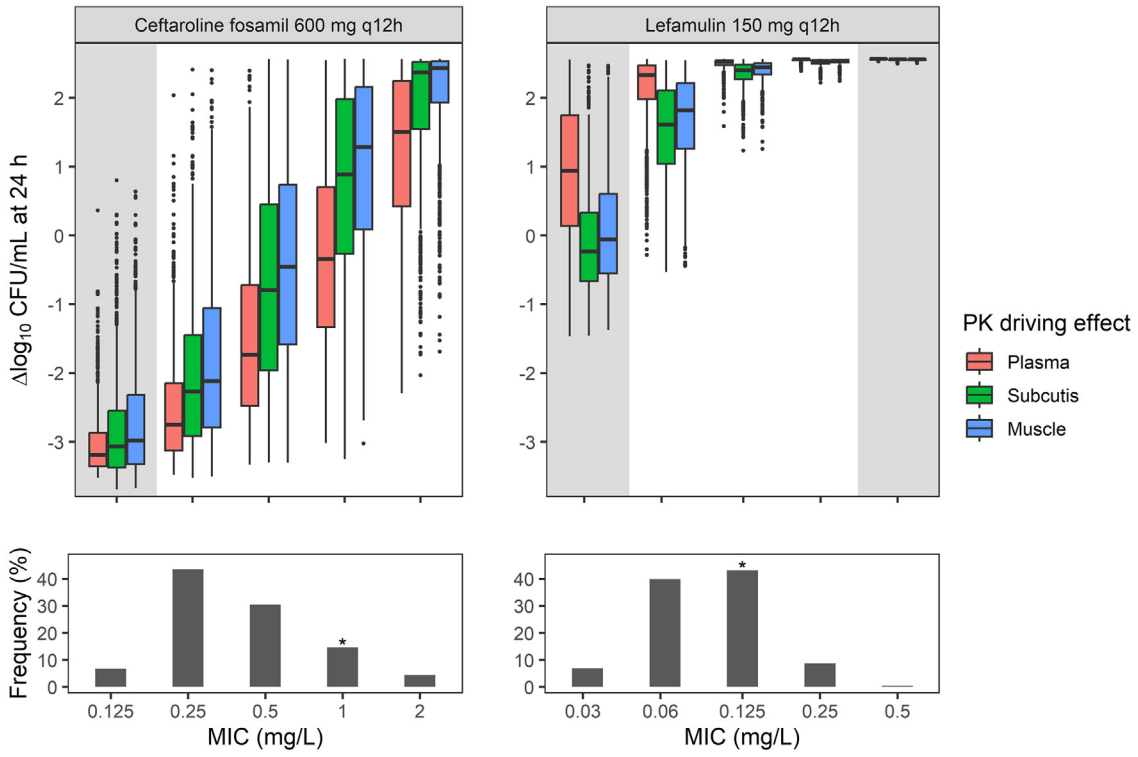

Figure 4. Antimicrobial effects of ceftaroline and lefamulin against MRSA with various MIC values given unbound concentrations in plasma and soft tissues. Top panels: log_{10}-change in CFU/mL at 24 h compared to baseline (10^6 CFU/mL) in simulations with different MIC values. The grey shading indicates simulations with MIC values outside the experimentally tested range. Simulated bacterial response was driven by simulated unbound drug concentrations in plasma and soft tissues following standard dosages. Boxplots indicate the median and interquartile range (IQR); whisker lengths cover the 25th/75th percentiles −/+ 1.5·IQR, and outliers outside that range are shown as filled circles. Bottom panels: relative MIC distributions, based on a total of 5429 and 10 181 observations for lefamulin and ceftaroline, respectively [34]. MIC_{90} values are marked with an asterisk. MIC values outside the displayed range are also recorded in the database and represent <1% of the total number of observations. MRSA: methicillin-resistant *Staphylococcus aureus*; MIC: minimum inhibitory concentration; CFU: colony-forming units; PK: pharmacokinetics.

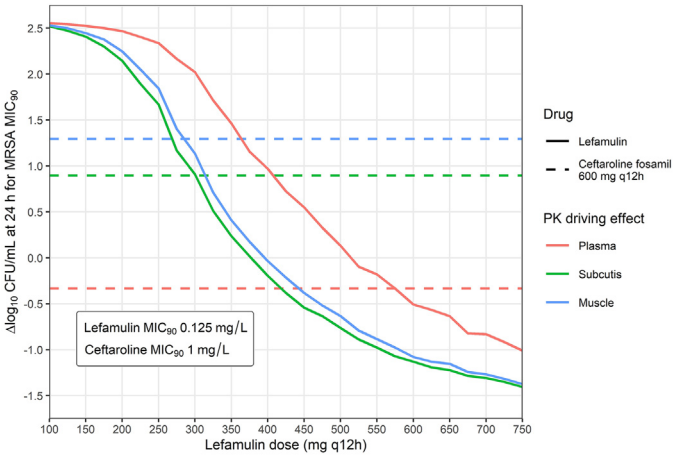

Figure 5. Lefamulin dosage required to match the antimicrobial effect of the standard dosage of ceftaroline given unbound concentrations in plasma and soft tissues and MRSA MIC_{90} values of both drugs. Lines represent the median log_{10}-change in CFU/mL at 24 h compared to baseline (10^6 CFU/mL) in simulations with the respective MRSA MIC_{90} for lefamulin and ceftaroline. The dose (x-axis) at which the dashed and the solid line of the same colour cross represents the lefamulin dosage at which the median predicted bacterial count at 24 h is equal to that following a standard dosage of ceftaroline fosamil. MRSA: methicillin-resistant *Staphylococcus aureus*; MIC: minimum inhibitory concentration; CFU: colony-forming units; PK: pharmacokinetics.

and antibiotic PK-PD [39]. Third, high spontaneous cure rates have been reported in trials with patients with SSTIs [40,41], making it difficult to determine the effect that can be ascribed to antibiotic treatment. Last, the time-kill experiments were performed over 24 h, which is not reflective of an entire course of antibiotic therapy. Informing the PK-PD model with time-kill data obtained over a longer period of time, e.g., using a hollow-fibre infection model, may provide more translational insights.

The microdialysis data underlying the PK models in this analysis were obtained in a limited number of healthy volunteers (n = 12 for both drugs). Apart from plasma PK, the tissue penetration of antibiotics may be altered or more variable in special populations, such as septic or obese patients [2,42]. In comparative PK-PD analyses like the one performed in this study, it is therefore important that the PK data for the drugs originated from similar populations. In absence of clinical PK data, simulations could be based on physiologically-based PK models.

The inclusion of MIC as a covariate on EC_{50} enabled the simultaneous description of all strains in the PD model and a power function was empirically selected to describe the relationship, as reported for other antimicrobial PK-PD models [23–26]. However, while covering 92% and 93% of the lefamulin and ceftaroline MIC values reported for MRSA by EUCAST [34], the range of MIC values of the studied strains was relatively narrow. Future studies should attempt to additionally include strains with less frequently occurring MIC values. This would allow for a better characterisation of potential relationships between the MIC and exposure-response parameters and for more accurate predictions across the entire MIC distribution. A limitation of using the MIC as a covariate is the limited precision associated with its determination [43], which might be propagated into the estimated covariate relationship. However, the MIC is the standard measure of antimicrobial susceptibility and MIC distributions commonly include abundant observations across different locations. Therefore, obtaining time-kill data using several strains with different MIC values and including the MIC as a

covariate in the PD model helps to place the simulations of bacterial response with the PK-PD model in a clinically relevant context. Additional limitations of this work include lacking genotypic information on the included isolates, as well as assessment of potential genotypic or phenotypic resistance development. Future analyses could track the emergence of resistant subpopulations over time through population analysis profiling to enable a comparison of antibiotics also regarding resistance development. Furthermore, genotypic and phenotypic data on resistance development could offer mechanistic insights to guide PD model development [44], rather than empirical model selection.

The PK-PD modelling approach applied in this work has several important advantages over using PK/PD index targets and PTA analyses to compare effect predictions of different antibiotics. First, it is based on concentrations at the target site of infection, i.e., the concentrations driving the antimicrobial effect, rather than solely relying on plasma concentrations. Second, it enables a 'head-to-head' comparison of effect against a specific pathogen of interest, whereas PK/PD index targets may have been derived using different sources of data, study designs, pathogens and endpoints, all of which may impact the selection of the appropriate PK/PD index and its magnitude [45]. Third, it considers and provides insight into the full time course and shape of antibiotic concentrations (PK) and bacterial growth and killing (PD) simultaneously, avoiding a loss of information associated with dichotomous measures like target attainment (yes/no) based on a summary PK/PD endpoint.

In conclusion, we demonstrated how target-site PK and in vitro PD data can be leveraged to predict and compare target site-specific antimicrobial effects. Given standard dosing regimens, ceftaroline appeared more effective against MRSA than lefamulin at soft-tissue concentrations. PK-PD modelling and simulation based on target-site concentrations could be used to inform antibiotic treatment and dosing strategies for specific indications and for comparisons of new with established treatment options, also in populations with altered (target-site) PK characteristics in whom large efficacy trials may be complicated to conduct.

Declarations

Funding: This work was supported by the European Union's Horizon 2020 Marie Skłodowska-Curie Actions research and innovation programme (grant number 861323).

Competing interests: None.

Ethical approval: Not required.

Sequence information: Not applicable.

Author contributions: Conceptualisation: WvO, MZ. Data collection and analysis: WvO, ADP, SE; Writing—Original Draft: WvO; Writing—Review & Editing: all authors; Supervision: MZ, IKM, JGCvH. All authors contributed to and approved submission of the final manuscript.

Supplementary materials

Supplementary material associated with this article can be found, in the online version, at doi:10.1016/j.ijantimicag.2024.107148.

References

[1] Jager NGL, van Hest RM, Lipman J, Roberts JA, Cotta MO. Antibiotic exposure at the site of infection: principles and assessment of tissue penetration. Expert Rev Clin Pharmacol 2019;12:623–34. doi:10.1080/17512433.2019.1621161.

[2] Joukhadar C, Frossard M, Mayer BX, Brunner M, Klein N, Siostrzonek P, et al. Impaired target site penetration of beta-lactams may account for therapeutic failure in patients with septic shock. Crit Care Med 2001;29:385–91. doi:10.1097/00003246-200102000-00030.

[3] Minichmayr IK, Schaeftlein A, Kuti JL, Zeitlinger M, Kloft C. Clinical determinants of target non-attainment of linezolid in plasma and interstitial space fluid: a pooled population pharmacokinetic analysis with focus on critically ill patients. Clin Pharmacokinet 2017;56:617–33. doi:10.1007/s40262-016-0463-7.

[4] van Os W, Zeitlinger M. Predicting antimicrobial activity at the target site: pharmacokinetic/pharmacodynamic indices versus time-kill approaches. Antibiotics 2021;10:1485. doi:10.3390/antibiotics10121485.

[5] Friberg LE. Pivotal role of translation in anti-infective development. Clin Pharm Therap 2021;109:856–66. doi:10.1002/cpt.2182.

[6] Cristinacce A, Wright JG, Macpherson M, Iaconis J, Das S. Comparing probability of target attainment against *Staphylococcus aureus* for ceftaroline fosamil, vancomycin, daptomycin, linezolid, and ceftriaxone in complicated skin and soft tissue infection using pharmacokinetic/pharmacodynamic models. Diagn Microbiol Infect Dis 2021;99:115292. doi:10.1016/j.diagmicrobio.2020.115292.

[7] Housman ST, Sutherland CA, Nicolau DP. Pharmacodynamic profile of commonly utilised parenteral therapies against meticillin-susceptible and meticillin-resistant *Staphylococcus aureus* collected from US hospitals. Int J Antimicrob Agents 2014;44:235–41. doi:10.1016/j.ijantimicag.2014.05.012.

[8] Sader HS, Biedenbach DJ, Paukner S, Ivezic-Schoenfeld Z, Jones RN. Antimicrobial activity of the investigational pleuromutilin compound BC-3781 tested against gram-positive organisms commonly associated with acute bacterial skin and skin structure infections. Antimicrob Agents Chemother 2012;56:1619–23. doi:10.1128/aac.05789-11.

[9] Prince WT, Ivezic-Schoenfeld Z, Lell C, Tack KJ, Novak R, Obermayr F, et al. Phase II clinical study of BC-3781, a pleuromutilin antibiotic, in treatment of patients with acute bacterial skin and skin structure infections. Antimicrob Agents Chemother 2013;57:2087–94. doi:10.1128/aac.02106-12.

[10] Kaye KS, Petty LA, Shorr AF, Zilberberg MD. Current epidemiology, etiology, and burden of acute skin infections in the United States. Clin Infect Dis 2019;68:S193–S1s9. doi:10.1093/cid/ciz002.

[11] Garau J, Ostermann H, Medina J, Ávila M, McBride K, Blasi F. Current management of patients hospitalized with complicated skin and soft tissue infections across Europe (2010–2011): assessment of clinical practice patterns and real-life effectiveness of antibiotics from the REACH study. Clin Microbiol Infect 2013;19:E377–EE85. doi:10.1111/1469-0691.12235.

[12] Zeitlinger M, Schwameis R, Burian A, Burian B, Matzneller P, Müller M, et al. Simultaneous assessment of the pharmacokinetics of a pleuromutilin, lefamulin, in plasma, soft tissues and pulmonary epithelial lining fluid. J Antimicrob Chemother 2016;71:1022–6. doi:10.1093/jac/dkv442.

[13] Beal SL. Ways to fit a PK model with some data below the quantification limit. J Pharmacokinet Pharmacodyn 2001;28:481–504. doi:10.1023/a:1012299115260.

[14] Rubino CM, Xue B, Bhavnani SM, Prince WT, Ivezic-Schoenfeld Z, Wicha WW, et al. Population pharmacokinetic analyses for BC-3781 using phase 2 data from patients with acute bacterial skin and skin structure infections. Antimicrob Agents Chemother 2015;59:282–8. doi:10.1128/aac.02033-13.

[15] Tunblad K, Hammarlund-Udenaes M, Jonsson EN. An integrated model for the analysis of pharmacokinetic data from microdialysis experiments. Pharm Res 2004;21:1698–707. doi:10.1023/b:pham.0000041468.00587.c6.

[16] Zhang L, Wicha WW, Bhavnani SM, Rubino CM. Prediction of lefamulin epithelial lining fluid penetration after intravenous and oral administration using Phase 1 data and population pharmacokinetics methods. J Antimicrob Chemother 2019;74:iii27–34. doi:10.1093/jac/dkz088.

[17] Helfer VE, Zavascki AP, Zeitlinger M, de Araújo BV, Dalla Costa T. Population pharmacokinetic modeling and probability of target attainment of ceftaroline in brain and soft tissues. Antimicrob Agents Chemother 2022;66:e00741e0022. doi:10.1128/aac.00741-22.

[18] Matzneller P, Lackner E, Lagler H, Wulkersdorfer B, Österreicher Z, Zeitlinger M. Single- and repeated-dose pharmacokinetics of ceftaroline in plasma and soft tissues of healthy volunteers for two different dosing regimens of ceftaroline fosamil. Antimicrob Agents Chemother 2016;60:3617–25. doi:10.1128/aac.00097-16.

[19] Chauzy A, Nadji A, Combes JC, Defrance N, Bouhemad B, Couet W, et al. Cerebrospinal fluid pharmacokinetics of ceftaroline in neurosurgical patients with an external ventricular drain. J Antimicrob Chemother 2019;74:675–81. doi:10.1093/jac/dky489.

[20] Van Wart SA, Forrest A, Khariton T, Rubino CM, Bhavnani SM, Reynolds DK, et al. Population pharmacokinetics of ceftaroline in patients with acute bacterial skin and skin structure infections or community-acquired bacterial pneumonia. J Clin Pharmacol 2013;53:1155–67. doi:10.1002/jcph.153.

[21] Clinical and Laboratory Standards Institute Performance standards for antimicrobial susceptibility testing. 30th ed. Wayne, PA: CLSI; 2020. M100.

[22] Tam VH, Schilling AN, Nikolaou M. Modelling time-kill studies to discern the pharmacodynamics of meropenem. J Antimicrob Chemother 2005;55:699–706. doi:10.1093/jac/dki086.

[23] Iqbal K, Broeker A, Nowak H, Rahmel T, Nussbaumer-Pröll A, Österreicher Z, et al. A pharmacometric approach to define target site-specific breakpoints for bacterial killing and resistance suppression integrating microdialysis, time-kill curves and heteroresistance data: a case study with moxifloxacin. Clin Microbiol Infect 2020;26:1255.e1–1255.e8. doi:10.1016/j.cmi.2020.02.013.

[24] Khan DD, Lagerbäck P, Cao S, Lustig U, Nielsen EI, Cars O, et al. A mechanism-based pharmacokinetic/pharmacodynamic model allows prediction of antibiotic killing from MIC values for WT and mutants. J Antimicrob Chemother 2015;70:3051–60. doi:10.1093/jac/dkv233.
[25] Yano Y, Oguma T, Nagata H, Sasaki S. Application of logistic growth model to pharmacodynamic analysis of in vitro bactericidal kinetics. J Pharm Sci 1998;87:1177–83. doi:10.1021/js9801337.
[26] Amann LF, Broeker A, Riedner M, Rohde H, Huang J, Nordmann P, et al. Pharmacokinetic/pharmacodynamic evaluation of tigecycline dosing in a hollow fiber infection model against clinical bla-KPC producing *Klebsiella pneumoniae* isolates. Diagn Microbiol Infect Dis 2024;108:116153. doi:10.1016/j.diagmicrobio.2023.116153.
[27] Food and Drug Administration Center for drug evaluation and research. Microbiology reviews. Application number: 200327. 2010. https://www.accessdata.fda.gov/drugsatfda_docs/nda/2010/200327orig1s000micror.pdf [accessed April 2023].
[28] Nguyen TH, Mouksassi MS, Holford N, Al-Huniti N, Freedman I, Hooker AC, et al. Model evaluation of continuous data pharmacometric models: metrics and graphics. CPT Pharmacometrics Syst Pharmacol 2017;6:87–109. doi:10.1002/psp4.12161.
[29] Lindbom L, Pihlgren P, Jonsson EN. PsN-Toolkit: a collection of computer intensive statistical methods for non-linear mixed effect modeling using NONMEM. Comput Methods Programs Biomed 2005;79:241–57. doi:10.1016/j.cmpb.2005.04.005.
[30] Keizer RJ, van Benten M, Beijnen JH, Schellens JHM, Huitema ADR. Piraña and PCluster: a modeling environment and cluster infrastructure for NONMEM. Comput Methods Programs Biomed 2011;101:72–9. doi:10.1016/j.cmpb.2010.04.018.
[31] R Core Team R: A language and environment for statistical computing. Vienna, Austria: R Foundation for Statistical Computing; 2022.
[32] Wicha WW, Strickmann DB, Paukner S. Pharmacokinetics/pharmacodynamics of lefamulin in a neutropenic murine pneumonia model with *Staphylococcus aureus* and *Streptococcus pneumoniae*. J Antimicrob Chemother 2019;74:iii11–iiii8. doi:10.1093/jac/dkz086.
[33] Shah DK, Betts AM. Towards a platform PBPK model to characterize the plasma and tissue disposition of monoclonal antibodies in preclinical species and human. J Pharmacokinet Pharmacodyn 2012;39:67–86. doi:10.1007/s10928-011-9232-2.
[34] European Committee on Antimicrobial Susceptibility Testing. MIC and zone distributions and ECOFFs. https://www.eucast.org/mic_distributions_and_ecoffs/ [accessed April 2023].
[35] European Medicines Agency. Assessment report Xenleta. 2020. https://www.ema.europa.eu/en/documents/assessment-report/xenleta-epar-public-assessment-report_en.pdf [accessed April 2023].
[36] Das S, Li J, Iaconis J, Zhou D, Stone GG, Yan JL, et al. Ceftaroline fosamil doses and breakpoints for *Staphylococcus aureus* in complicated skin and soft tissue infections. J Antimicrob Chemother 2019;74:425–31. doi:10.1093/jac/dky439.
[37] van Os W, Zeitlinger M. Target attainment of intravenous lefamulin for treatment of acute bacterial skin and skin structure infections. J Antimicrob Chemother 2024;79:443–6. doi:10.1093/jac/dkad401.
[38] Dalhoff A. Differences between bacteria grown in vitro and in vivo. J Antimicrob Chemother 1985;15(Suppl A):175–95. doi:10.1093/jac/15.suppl_a.175.
[39] van Os W, Wulkersdorfer B, Eberl S, Oesterreicher Z, Schwabl P, Reiberger T, et al. Bacterial growth and ceftriaxone activity in individual ascitic fluids in an in vitro model of spontaneous bacterial peritonitis. Front Pharmacol 2023;14:1124821. doi:10.3389/fphar.2023.1124821.
[40] Spellberg B, Talbot GH, Boucher HW, Bradley JS, Gilbert D, Scheld WM, et al. Antimicrobial agents for complicated skin and skin-structure infections: justification of noninferiority margins in the absence of placebo-controlled trials. Clin Infect Dis 2009;49:383–91. doi:10.1086/600296.
[41] Rajendran PM, Young D, Maurer T, Chambers H, Perdreau-Remington F, Ro P, et al. Randomized, double-blind, placebo-controlled trial of cephalexin for treatment of uncomplicated skin abscesses in a population at risk for community-acquired methicillin-resistant *Staphylococcus aureus* infection. Antimicrob Agents Chemother 2007;51:4044–8. doi:10.1128/aac.00377-07.
[42] Ehmann L, Simon P, Busse D, Petroff D, Dorn C, Huisinga W, et al. Risk of target non-attainment in obese compared to non-obese patients in calculated linezolid therapy. Clin Microbiol Infect 2020;26:1222–8. doi:10.1016/j.cmi.2020.04.009.
[43] Mouton JW, Muller AE, Canton R, Giske CG, Kahlmeter G, Turnidge J. MIC-based dose adjustment: facts and fables. J Antimicrob Chemother 2017;73:564–8. doi:10.1093/jac/dkx427.
[44] Jacobs M, Grégoire N, Couet W, Bulitta JB. Distinguishing antimicrobial models with different resistance mechanisms via population pharmacodynamic modeling. PLoS Comput Biol 2016;12:e1004782. doi:10.1371/journal.pcbi.1004782.
[45] Nielsen EI, Cars O, Friberg LE. Pharmacokinetic/pharmacodynamic (PK/PD) indices of antibiotics predicted by a semimechanistic PKPD model: a step toward model-based dose optimization. Antimicrob Agents Chemother 2011;55:4619–30. doi:10.1128/AAC.00182-11.